# Detailed investigation of the reduction process of cupric oxide (CuO) to form metallic copper fine particles with a unique diameter

**Tetsu Yonezawa · Atsushi Hyono · Naoki Nishida**

**Abstract** Copper fine particles were successfully prepared by hydrazine reduction of cupric oxide (CuO). Changes in the temperature and pH values during the redox reaction of cupric oxide and hydrazine monohydrate were observed in detail. These changes reflected the reaction steps leading to the formation of metallic copper particles. The reduction of cupric oxide proceeded mainly during the part of the process where the pH value changes little or only very slowly. This phenomenon strongly indicates that the reaction and the particle structures can be established by control of the pH during the formation.

## Introduction

During the past few decades, nanotechnologies have been intensively investigated due to strong interest by many researches and engineers [1–7]. In particular, metal nano-/fine-particles have attracted interest because of their unique properties resulting from their particle sizes. The lower melting points as well as high catalytic properties of such particles have been considered useful properties in industrial applications, and localized surface plasmon resonance (LSPR) and surface-enhanced Raman spectroscopy (SERS) of gold, silver, and copper particles can contribute to create highly sensitive sensors, especially for biosensing [8–15]. Copper nano- and fine-particles have also attracted interest in applications with electroconductive pastes for wiring or

thin electrodes [16], e.g., as the inner electrodes of multi-layered ceramic capacitor (MLCC) [17].

A wide variety of procedures for the preparation of metal nano- and fine-particles with desirable sizes, shapes, and compositions have been reported including evaporation of metal atoms, chemical reduction of metal ions [2–5, 16, 18–21], as well as solve-thermal processes have been developed [4]. Among these, chemical reduction is considered one of the most important and simple methods of preparation, because the properties of the obtained particles can be readily controlled by varying reduction conditions including the choice of the metal source salts, educing reagents, stabilizers, reduction temperatures, concentrations, and other parameters [2–5, 15–17]. Chemical reduction is usually propagated by introducing a reductant into a homogeneous solution of metal ions with the aim of producing a homogeneous supersaturated solution of metal atoms. The particle preparation process consists of a nucleation stage followed by a particle growth stage. In both the stages, metal atoms precipitate from the supersaturated solution of metal atoms generated during the reduction process. To obtain controlled and uniform-sized particles, this precipitation process must be precisely controlled, and it is necessary to know how and when the nuclei are formed and how they grow throughout the preparation process.

Recently, we have reported a preparation procedure of copper particles by hydrazine reduction of cupric oxide (CuO) [21]. The metal source, cupric oxide, is a solid and homogeneous metal ion solution was not used as the precursor. However, this process resulted in unique particle sizes. In the report here, the pH and the temperature during the preparation of copper fine particles from cupric oxide by the redox reaction with hydrazine monohydrate was observed in detail, and the relationship between the pH

T. Yonezawa (✉) · A. Hyono · N. Nishida
Division of Materials Science and Engineering, Faculty of
Engineering, Hokkaido University, Kita13, Nishi8, Kita-ku,
Sapporo, Hokkaido 060-8628, Japan
e-mail: tetsu@eng.hokudai.ac.jp

value and the precipitation stages of copper will be discussed.

## Experimental

### Materials

Cupric oxide (CuO) was purchased from Nisshin Chemco Co., Japan. Hydrazine monohydrate, ammonia aqueous solution (28%), and ethanol (GR grade) were purchased from Kanto Chemical and used without further purification. Water was twice distilled and then purified by a Milipore Simplicity or an Organo/ELGA Purelabo system (>18 MΩ). Gelatin was supplied from Nitta Gelatin Co., Japan.

### Apparatus

Temperatures were monitored with a temperature logger equipped with a K-type thermocouple, and pH values were monitored with a Toa-DKK pH meter. Some samples were centrifuged with a Hitachi GX-150 Ultracentrifuge (80000 rpm). The particle structure was observed with a field-emission-type scanning electron microscope, JEOL JSM-6701F with an acceleration voltage of 15 kV, X-ray diffraction (XRD) patterns were obtained with a Philips X'PERT, equipped with a Cu Kα tube, and reaction status was recorded with a digital camera.

### Generation of copper particles

All glass vessels were scratch-free on the inside surfaces to avoid polydispersity of particles, and the vessels were cleaned with aqua rigia and rinsed thoroughly with pure water before the experiments to eliminate organic/inorganic contamination. The reduction process for producing the copper particles is a modification of the reported in [21]. Here, 500 cm$^3$ of water and an equal volume of ethanol were introduced into a 2-dm$^3$ round-bottomed flask with four necks, after which 32 g of gelatin was completely dissolved in the mixture. Then, 80 g of cupric oxide powder (1 mol) was suspended in this solution and 36 cm$^3$ of 2-aminoethanol (complex reagent) was added, 70 cm$^3$ of ammonia aqueous solution (28%) was introduced to adjust pH to 10.5–11. With 2-aminoethanol and ammonia, cupric ions form complexes and dissolve into the solution. A temperature logger with a K-type thermocouple and a pH meter were attached to this reaction flask. The solution was then stirred by a magnetic stirrer and heated in an oil bath to 60 °C. Hydrazine monohydrate solution was introduced all at once into the CuO suspension. At the point when pH value stopped to decrease (mentioned later, position 2 in

Fig. 1), the flask was heated up to 80 °C for complete reduction of cupric oxide to metallic copper. The temperature and pH value were monitored for 2 h, from putting hydrazine monohydrate until stop heating.

### Characterization of the copper particles

During the reaction, four small portions, 20–30 cm$^3$, were removed from the reaction suspension, at times which will be detailed in the following section. These portions were immediately cooled in an ice bath to discontinue the reduction process. The cooled solution volumes were centrifuged to obtain the solid particles formed during the reduction to elucidate the reduction process in detail. After the reaction, the products were filtered over a membrane filter (0.45 μm Omnipore, Millipore) and washed with purified water. The particles were then dried flowing N$_2$ at 60 °C for 1 h in a tube furnace. The obtained particles were observed with a scanning electron microscope and their XRD patterns were determined.

## Results and discussion

### Temperature and pH changes during the reduction

The time courses of the temperature and pH of the CuO suspension in the reaction flask in the presence of gelatin during the reduction by hydrazine are shown in Fig. 1. Injection of hydrazine monohydrate is at $t = 0$ and the progress of the reaction is divided into five stages, as
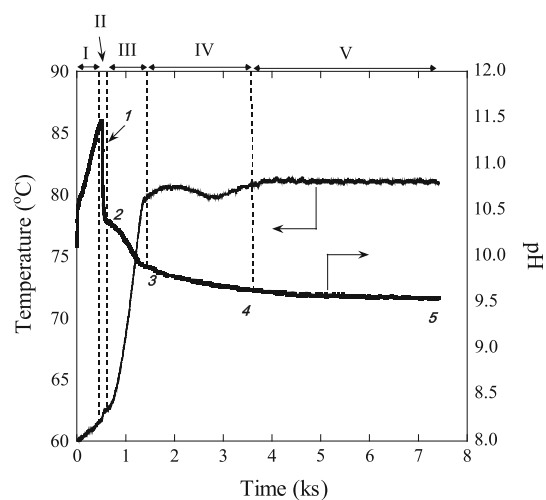


**Fig. 1** Changes in the temperature (*thin curve*, left ordinate) and pH value (*thick curve*, right ordinate) during the reduction of cupric oxide (CuO) by hydrazine monohydrate. Injection time of hydrazine monohydrate at $t = 0$. Details of the various numbers are presented in the "Results and discussion" (temperature and pH changes during the reduction section)

below, for a better understanding of copper fine particle formation process.

Stage I: from the start of the experiment till the point of the highest pH value. (0 < $t$ < 490 s).

Stage II: from the point with the highest pH value to first break in the descending pH curve where the second period of heating of the flask was started (490 s < $t$ < 590 s).

Stage III: up to the second break in the decrease in pH during the heating to 80 °C (590 s < $t$ < 1520 s).

Stage IV: from the time when the temperature reached about 80 °C, and where the gradual decrease pH flattens out further (1520 s < $t$ < 3600 s).

Stage V: final practically flat pH region (3600 s < $t$ < 7200 s).

At the start of the reaction, the pH increased dramatically (Stage I) to 11.5, and then it rapidly decreased to the initial value and with a short less rapid decrease (Stage II). During the second heating from 60 to 80 °C, the pH value decreased very gradually to 9.9 (Stage III) and after the temperature reached 80 °C, it remained very nearly constant (Stages IV and V).

Small sample portions, 20–30 cm$^3$, were removed from the reaction suspension at the following four times and the solid products were separated by ultracentrifuge with the fifth sample consisting of the final product remaining in the flask:

(1) in Stage II, at pH 11.2 while the pH is decreasing ($t$ = 530 s),

(2) in Stage III, between the end of the first rapid pH decrease and at the start of the second heating (first pH knee point) ($t$ = 590 s),

(3) in Stage IV, when the temperature reached 80 °C ($t$ = 1520 s),

(4) in Stage IV, about 1 h after the hydrazine monohydrate addition ($t$ = 3680 s), and

(5) in Stage V, 2 h after the hydrazine monohydrate addition ($t$ = 7200 s, the final product).

Gas was vigorously generated just after injection of hydrazine into the CuO suspension (Stage I) and also during Stage III. Figure 2 shows photographs of the solution in the reaction flask at different stages during the reduction of the cupric oxide. As can be seen the liquid in the reaction flask in Stage I ($t$ = 110 s, Fig. 2a) and Stage III (point 2 in Fig. 1, $t$ = 590 s, Fig. 2c), appears foggy (semi opaque) in the upper part of the flask. These images correspond to the vigorous gas evolution stages. Small bubbles are also observed on the surface of the black suspension in Stage II (point 1, $t$ = 530 s, Fig. 2b). This gas evolution can be attributed to a hydrazine oxidation reaction as will be described below (Eq. 1). Reduction of CuO by hydrazine without ethanol was also attempted. Here, the bubbles grew agitatedly and finally overflowed even a 5-dm$^3$ beaker (with the reaction suspension 1 dm$^3$) during the Stage I. Further, with the formation of large bubbles, the reaction suspension became inhomogeneous and the uniform stirring of the suspension could not be achieved. In this situation, the obtained metallic copper particles showed a wide size distribution. To avoid the occurrence of this kind of bubbles, alcohols or other surfactants are indispensable for the
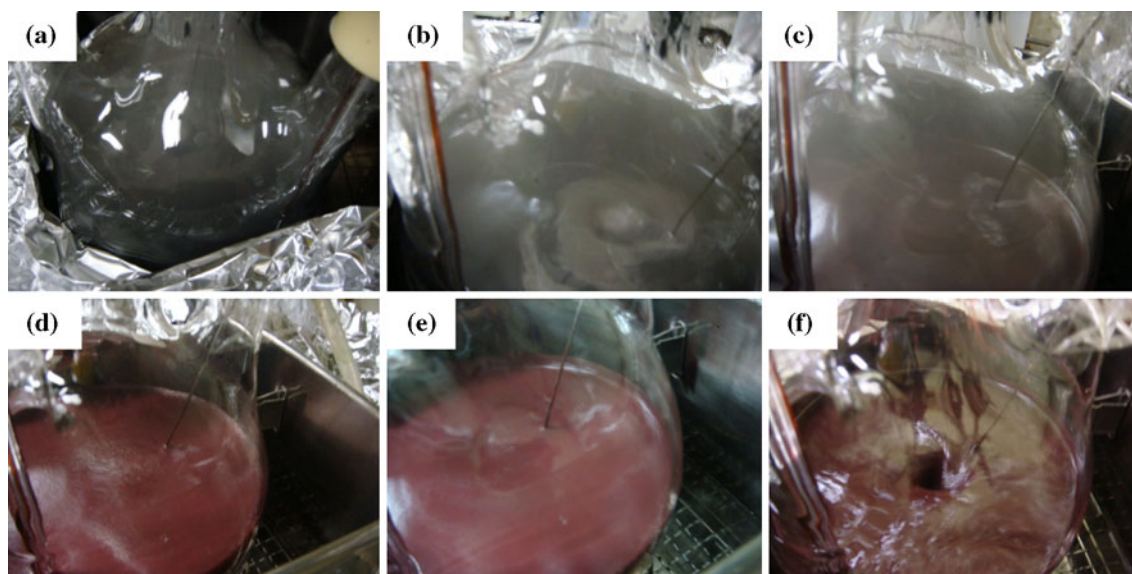


**Fig. 2** Photographs of the reaction flask during the hydrazine reduction of cupric oxide to metallic copper. **a** Stage I, $t$ = 110 s; **b** point 1 in Stage II, $t$ = 530 s; **c** point 2 in Stage III, $t$ = 590 s; **d** point 3 in Stage III, $t$ = 1520 s; **e** point 4 in Stage IV, $t$ = 3680 s; and **f** dispersion of the final product, $t$ = 7200 s. For details of the stages and points please refer to Fig. 1 and the "Results and discussion"

reaction process as an anti-bubble reagent. In Stages IV and V, gas continued to be generated gently and without the violence of Stages I and III, suggesting that the reduction was progressing, although more slowly.

The color of the reaction suspension is an indicator of the progress of the reaction. Figure 2c shows a slightly red color (point 2 in Fig. 1), suggesting the formation of copper particles in this suspension. A considerable color change of the reaction suspension from black to dark red can be observed in Fig. 2d (point 3). The black color corresponds to cupric oxide (CuO) and metallic copper particles with the diameter of ca. 100 nm are a cause of the dark red color. This color change strongly suggests that at point 3 (Fig. 1), metallic copper is the main product. Two hours after the addition of hydrazine, no cupric oxide was observed. Formation of cuprous oxide ($Cu_2O$) during the process could not be established by these color changes, because cuprous oxide shows as orange.

### SEM observations and XRD patterns of the products

A SEM image of the cupric oxide powder used as the metal source is shown in Fig. 3a. The SEM images in Fig. 3b–f show the particles obtained by centrifugation of the suspensions removed during the reaction and Fig. 3g is the SEM image of the copper particles in the final product. Figure 3h, i, and j are the SEM images in Fig. 3b, f, and g, respectively, in a higher magnification. The SEM images allow a ready distinguishing of the cupric oxide (micron sized) and produced copper particles ($\sim$100-nm class, spherical) from their sizes and structures observed.

Cupric oxide (CuO) particles with sizes above 1 μm can be observed from the start of the reaction to point 3 in Fig. 1 (Fig. 3b–d). At points 4 (Fig. 3e) and 5 (Fig. 3f) particles with diameters of ca. 100 nm are observed without larger particles present. The XRD patterns are shown in Fig. 4, and the letters correspond to the SEM images.

The XRD patterns of the particles from the samples removed at points 1 and 2 in Fig. 1 (Fig. 4b, c) predominantly show diffraction peaks of cupric oxide, and only small peaks for metallic copper. The peak at $2\theta = 42°$ in Fig. 4b is quite small and is slightly broadened, probably due to the smallness of the metallic copper particles. The XRD peaks of the particles from the samples removed at the point 3 of Fig. 1 (Fig. 4d) clearly indicate that there has been growth of the metallic copper particles. In the SEM images of the particles from the samples removed at points of 1 and 2 in Fig. 1 (Fig. 3b, c), there are small particles with diameters of 50–100 nm on the larger micron-sized particles, as can be seen in Fig. 3h. These particles may be
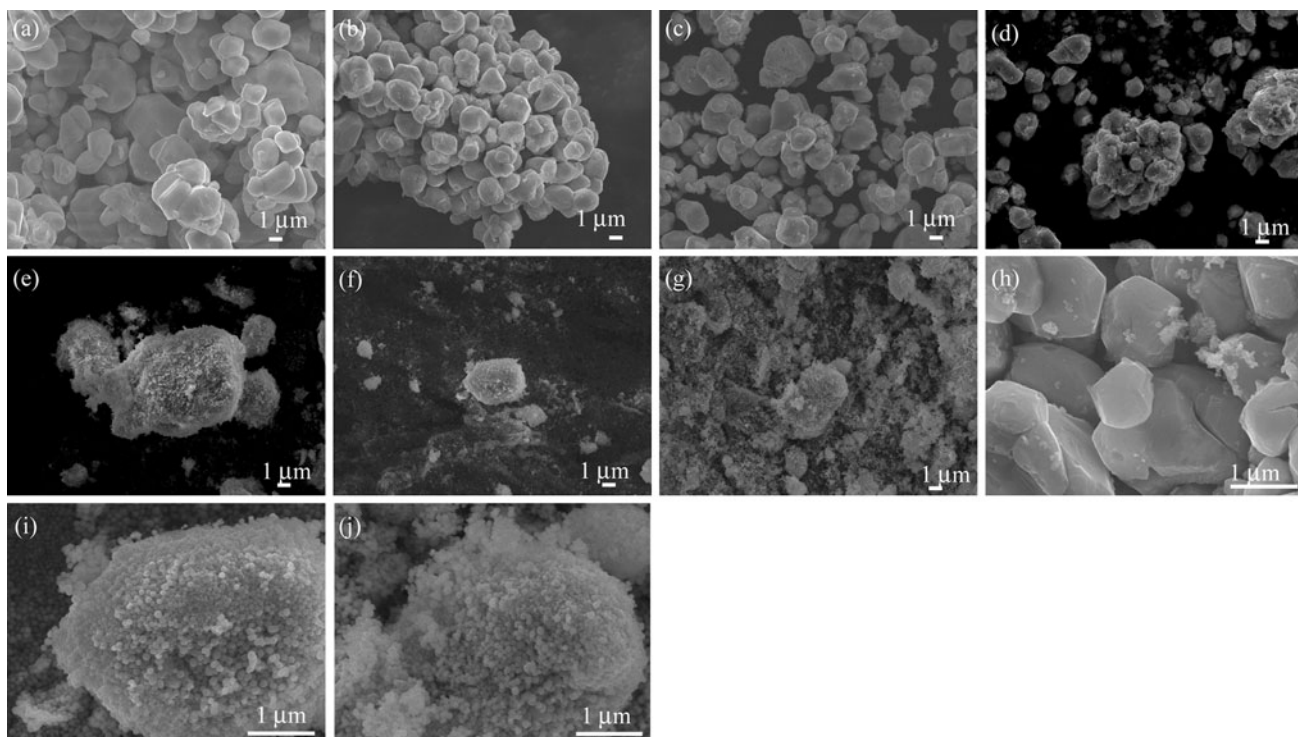


**Fig. 3** Scanning electron microscopic images of **a** the cupric oxide (CuO) powders as received (metal sauce), **b–f** the solid parts of the suspension removed from the reaction suspension at points 1 (**b**), 2 (**c**), 3 (**d**), 4 (**e**), 5 (**f**), and **g** the final product. **h**, **i**, and **j** are the images as in the same samples of **b**, **f**, and **g**, respectively, with a higher magnification. For details of the points please refer to Fig. 1 and the "Results and discussion"
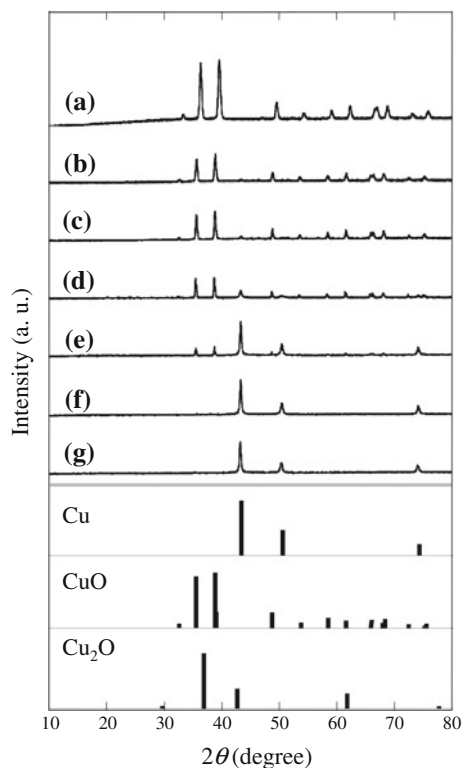
**Fig. 4** X-ray diffraction patterns of (*a*) the cupric oxide powders as received (metal sauce), (*b*)–(*f*) the solid parts of the suspension removed from the reaction suspension at points 1 (*b*), 2 (*c*), 3 (*d*), and 4 (*e*), 5 (*f*), and (*g*) the final product. Standard diffraction patterns of copper are shown in the three bottom spectra. For details of the points please refer to Fig. 1 and the "Results and discussion"

considered metallic copper particles, but the amount of these smaller particles is quite limited. In Fig. 3d (point 3 in Fig. 1), 100-nm particles are observed and the oxide particles have become smaller. In Fig. 3e (point 4), 100-nm copper fine particles are mainly observed. This SEM image clearly suggests that reduction of cupric oxide to metallic copper proceeded during Stage III but that it was not complete at point 3, even when the color of the reaction suspension was dark red.

The XRD pattern (Fig. 4e) of the particles from the samples removed at point 4 (Fig. 1) shows that these particles are mainly metallic copper and that a small amount of cupric oxide remains. The XRD pattern of the final product shows that there were only metallic copper particles in the solution. The phenomena described here correspond well to the conditions observed in the enlarged SEM images (Fig. 3e, f). This allows the surmise that two hours of heating at 80 °C completed the hydrazine reduction of cupric oxide to metallic copper.
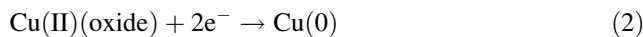
None of the XRD spectra showed any evidence of the existence of cuprous oxide ($Cu_2O$) in the solutions. As will be shown below, cupric ions would be reduced directly to metallic copper by four electron oxidation of hydrazine (Eqs. 1–4).
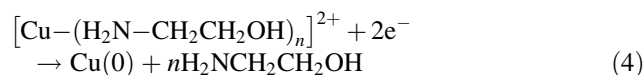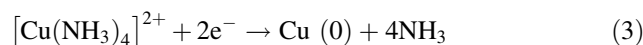
## Relation between the pH value and the oxidation–reduction

In electrochemistry, it is generally accepted that [22, 23] oxidation of hydrazine in alkaline solution is expressed as follows:

$$N_2H_4 + 4OH^- \rightarrow N_2 + 4\ H_2O + 4\ e^- \tag{1}$$
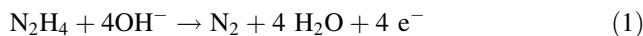
The electrons generated through Eq. 1 reduce cupric ions ($Cu^{2+}$) to metallic copper. As the reaction was carried out under alkaline conditions by the addition of ammonia solution, the metal source could be in two forms as below.

$$Cu(II)(oxide) + 2e^- \rightarrow Cu(0) \tag{2}$$

or

$$\left[Cu(NH_3)_4\right]^{2+} + 2e^- \rightarrow Cu\ (0) + 4NH_3 \tag{3}$$

$$\begin{aligned}\left[Cu-(H_2N-CH_2CH_2OH)_n\right]^{2+} &+ 2e^- \\ &\rightarrow Cu(0) + nH_2NCH_2CH_2OH\end{aligned} \tag{4}$$

Considering reaction equations 1–4, the reduction of copper leads to nitrogen gas generation and decreases in the pH value. The total volume of nitrogen gas generated during this reaction in the reactions reported here would be 11.2 $dm^3$ (0.5 mol, half of the amount of CuO (1 mol)). During the reaction, gas was generated vigorously in Stages I and III, and some gas was also generated in Stages IV and V. The pH values decreased from Stage II to IV and remained nearly almost constant in Stage V.

As mentioned above, from Stage II there were smaller spherical particles, assumed to be metallic copper particles, in the SEM images (Fig. 3b–f). The XRD peaks corresponding to metallic copper are quite small in Fig. 4b and c (at points 2 and 3 in Fig. 1), corresponding to Stages I–III. The peaks of copper particles in XRD patterns clearly appear after point 3, i.e., after Stage III (Fig. 4d). Comparing the XRD patterns of the particles at points 3 and 4 of Fig. 1 (Fig. 4d, e) suggests that most of cupric oxide was reduced to metallic copper in Stage IV. Then, in Stage V, where almost no change of the pH value was observed, the reduction of cupric ions was complete.

To explain the variations in the pH values, SEM images, and XRD patterns during the reduction process, it is necessary to consider that two or more reactions proceed simultaneously. Directly after the injection of hydrazine monohydrate to the CuO suspension, cupric ions forming complexes with ammonia or aminoethanol were quickly reduced as described by Eqs. 3 and 4. With the rapid reaction in Stage II, pH decreased abruptly (11.5 → 10.4) over a very short time. However, the amount of decrease in the hydroxyl ions in Stage II is $\sim 10^{-3}$ mol, which is much less than the total amount of source metal (cupric oxide), about 1 mol. Therefore, most of cupric oxide would still remain at point 3

(at the end of the Stage III in Fig. 1). This is confirmed with the SEM image (Fig. 3d) and the XRD pattern (Fig. 4d).

In Stages IV and V, the reduction reaction of cupric oxide to metallic copper proceeded without any considerable pH change. In this period, the equilibrium with hydroxyl ions may be assumed to be achieved by hydroxyl ions supplied by the weak alkaline conditions, i.e., ammonium molecules or copper(II) ammonia complexes, which had been added to maintain the alkalinity of the suspension:

$$NH_3 + H_2O \rightarrow NH_4^+ + OH^- \qquad (5)$$
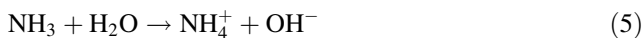
Some gas generation continued also in Stages IV and V. As noted above, the total volume of evolved gas is 11.2 dm$^3$ in the reaction reported here. The vigorous gas evolution in Stage I is due to the rapid reaction of the solvated copper complexes initially generated during the mixing of the suspension compounds, and this instant gas evolution made the bubbles in the flask large. In Stages IV and V, the reduction occurred directly on the surface of cupric oxide powders or with the copper complexes solvated by free NH$_3$ or amine molecules. Therefore, the gas generation at these stages was without formation of large bubbles.

These phenomena may all contribute to the uniformly sized copper particle formation reported in this study.

Figure 5 is a schematic illustration of the reduction process reported here and suggests the reasons for the formation of the uniformly sized copper particles. At the initial step, the generation of metallic copper atoms happens instantaneously when hydrazine monohydrate is injected into the reaction suspension. The result would be the formation of a supersaturated solution of metallic copper atoms. Then, these copper atoms aggregate to from copper nuclei. After that, copper atoms are produced by surface reactions, which are relatively slower than the reactions in the step, and the copper atoms deposit on the previously formed copper nuclei [1, 4]. It may be expected that control of the reaction rate in the pH equilibrium would enable control of the nuclei growth rate of particles, which would enable production of specified sizes of particles.

## Conclusion

The changes in temperature and pH values during the reduction–oxidation reaction of cupric oxide (CuO) and hydrazine monohydrate were observed in detail in this report. The results of the observations indicate that the reduction rate of Cu$^{2+}$ to Cu(0) changes during the
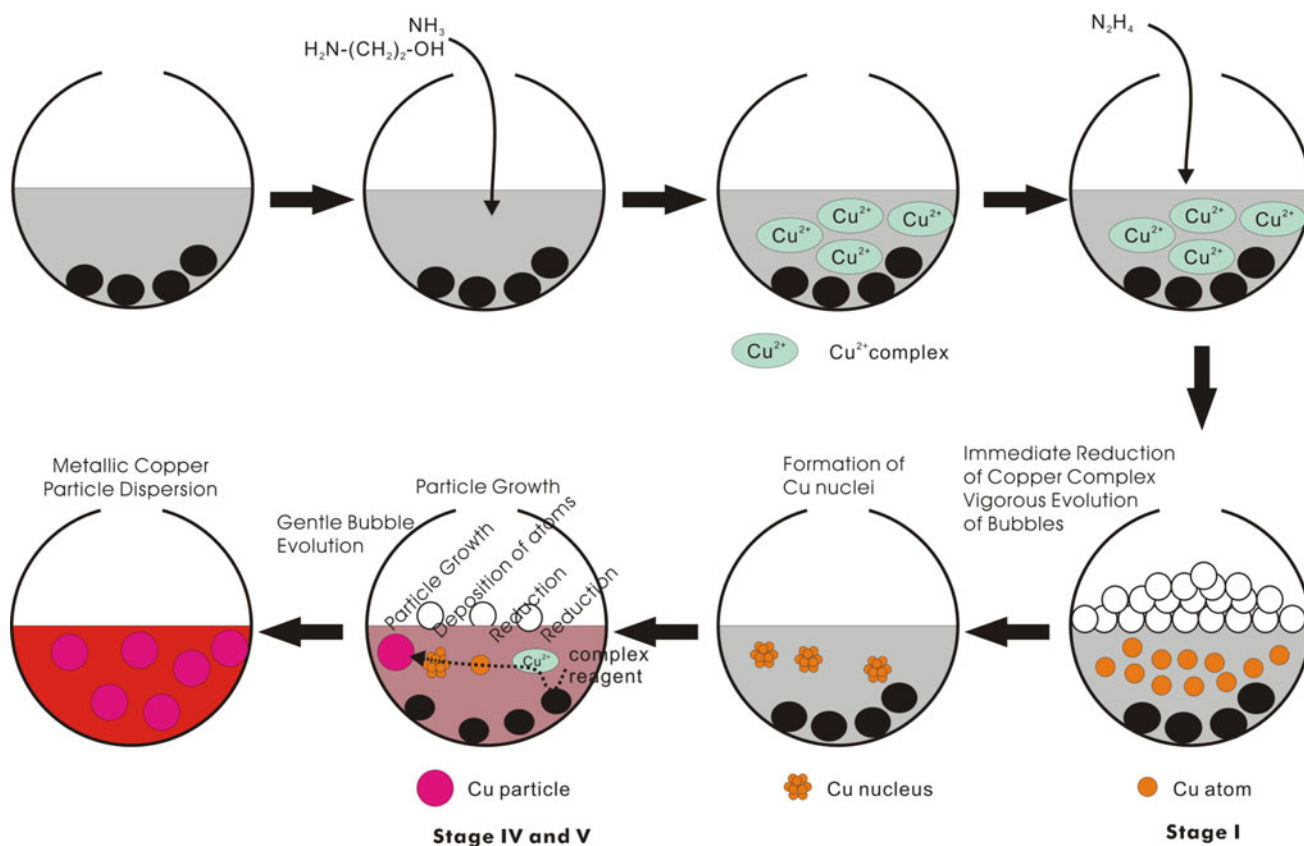


**Fig. 5** Schematic illustration of the formation process of metallic copper particles from cupric oxide in alkaline condition by hydrazine reduction as reported in this article

observed reaction. There is a rapid reduction of cupric ions at the injection of hydrazine resulting in copper nuclei formation and then a slower reduction of CuO enabled the growth of these nuclei to copper particles. This study clearly shows that pH control is an important factor in the formation of copper particles of specific sizes.

## References

1. Schmid G (1994) Clusters and colloids. VCH, Weinheim
2. Pileni MP (2003) Nat Mater 2:145
3. Toshima N, Yonezawa T (1998) New J Chem 22:1179
4. Burda C, Chen X, Narayanan R, El-Sayed MA (2005) Chem Rev 105:1025
5. Hodes G (2007) Adv Mater 19:639
6. Albrecht MA, Evans CW, Raston CL (2006) Green Chem 8:417
7. Wei H, Li B, Wang E, Dong S (2007) Chem Commun 3735
8. Lu X, Rycenga M, Skrabalak SE, Wiley B, Xia Y (2009) Annu Rev Phys Chem 60:167
9. Narayanan R, El-sayed MA (2005) J Phys Chem B 109:18460
10. Davis TJ, Vernon KC, Gómez DE (2009) Phys Rev B 79:155423
11. Jain PK, Huang X, El-Sayed IH, El-Sayed MA (2008) Acc Chem Res 41:1578
12. Tsung CK, Kuhn JN, Huang W, Aliaga C, Hung LI, Somorjai GA, Yang P (2009) J Am Chem Soc 131:5816
13. Nakamula I, Yamanoi Y, Yonezawa T, Imaoka T, Yamamoto K, Nishihara H (2008) Chem Commun 44:5716
14. Toshima N, Yonezawa T, Kushihashi K (1995) J Chem Soc Faraday Trans 89:2537
15. Tian C, Mao B, Wang E, Kang Z, Song Y, Wang C, Li S, Xu L (2007) Nanotechnology 18:285607
16. Lee Y, Choi J-r, Lee KJ, Stott NE, Kim D (2008) Nanotechnology 19:415604
17. Yonezawa T, Takeoka S, Kishi H, Ida K, Tomonari M (2008) Nanotechnology 19:145706
18. Ren X, Dong C, Tang F (2005) J Phys Chem B 109:15803
19. Chang Y, Lye ML, Zeng HC (2005) Langmuir 21:3746
20. He Y, Yu X, Yang B (2006) Mater Chem Phys 99:295
21. Tomonari M, Ida K, Yamashita H, Yonezawa T (2008) J Nanosci Nanotechnol 8:2468
22. Iida H, Nakanishi T, Takada H, Osaka T (2006) Electrochim Acta 52:292
23. Yin WX, Li ZP, Zhu JK, Qin HY (2008) J Power Sour 182:520